Journal of Medicinal Chemistry

ARTICLE

pubs.acs.org/jmc

Indolylarylsulfones as HIV-1 Non-Nucleoside Reverse Transcriptase Inhibitors: New Cyclic Substituents at Indole-2-carboxamide

Giuseppe La Regina,[†] Antonio Coluccia,[†] Andrea Brancale,[‡] Francesco Piscitelli,[†] Valerio Gatti,[†] Giovanni Maga,[§] Alberta Samuele,[§] Christophe Pannecouque,[⊥] Dominique Schols,[⊥] Jan Balzarini,[⊥] Ettore Novellino,[‖] and Romano Silvestri*[,†]

[†]Istituto Pasteur - Fondazione Cenci Bolognetti, Dipartimento di Chimica e Tecnologie del Farmaco, Sapienza Università di Roma, Piazzale Aldo Moro 5, I-00185 Roma, Italy

[‡]Welsh School of Pharmacy, Cardiff University, King Edward VII Avenue, Cardiff CF10 3NB, U.K.

[§]Istituto di Genetica Molecolare, Consiglio Nazionale delle Ricerche, Via Abbiategrasso 207, I-27100 Pavia, Italy

[‖]Dipartimento di Chimica Farmaceutica e Tossicologica, Università di Napoli Federico II, Via Domenico Montesano 49, I-80131, Napoli, Italy

[⊥]Rega Institute for Medical Research, Katholieke Universiteit Leuven, B-3000 Leuven, Belgium

S Supporting Information

ABSTRACT: New indolylarylsulfone derivatives bearing cyclic substituents at indole-2-carboxamide linked through a methylene/ethylene spacer were potent inhibitors of the WT HIV-1 replication in CEM and PBMC cells with inhibitory concentrations in the low nanomolar range. Against the mutant L100I and K103N RT HIV-1 strains in MT-4 cells, compounds **20**, **24**−**26**, **36**, and **40** showed antiviral potency superior to that of NVP and EFV. Against these mutant strains, derivatives **20**, **24**−**26**, and **40** were equipotent to ETV. Molecular docking experiments on this novel series of IAS analogues have also suggested that the H-bond interaction between the nitrogen atom in the carboxamide chain of IAS and Glu138:B is important in the binding of these compounds. These results are in accordance with the experimental data obtained on the WT and on the mutant HIV-1 strains tested.

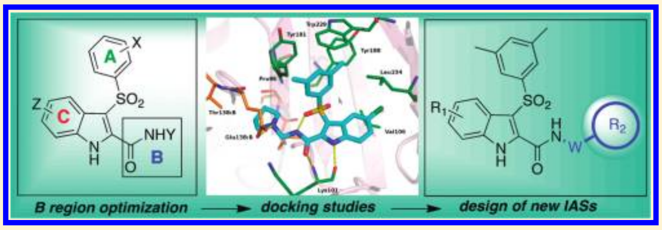

INTRODUCTION

Human immunodeficiency virus (HIV) was identified as the causative agent of acquired immunodeficiency syndrome (AIDS) in 1983.[1] Although significant progress has been made in the prevention and treatment of AIDS/HIV infection over the past 20 years, the number of people living with HIV is constantly growing. Worldwide, AIDS-related diseases are still one of the leading causes of death and are predicted to cause significantly premature mortality in the coming decades.[2]

HIV drugs currently approved by Food and Drug Administration (FDA) fall into seven target classes: nucleoside reverse transcriptase inhibitors (NRTIs), nucleotide reverse transcriptase inhibitors (NtRTIs), non-nucleoside reverse transcriptase inhibitors (NNRTIs), protease inhibitors (PIs), fusion inhibitors (FIs), CCR5 co-receptor inhibitors (CRIs), and integrase inhibitors (INIs).[3] Highly active antiretroviral therapy (HAART) combines three (recommended) or four different antiretroviral drugs. HAART regimes slow viral replication and reduce plasma viremia below the detection level, resulting in a substantial delay of disease progression.[4] However, long-term HAART treatments lead to the emergence of complications due to drug resistance,[5] toxicity, and adverse effects.[6] A major concern of earlier NNRTIs was the rapid development of drug resistance; in particular, K103N and Y181C were the most prevalent mutations in clinical HIV-1 isolates.[7] Therefore, new NNRTIs that display a broad spectrum of activity against clinically relevant HIV-1 mutant strains are needed. New generation NNRTIs are currently ongoing clinical trials.[8] Among them, etravirine (ETV) was approved for drug combination treatment of HIV-1 infected people who experienced drug resistance to other drugs of this class.[9]

Our efforts have been focused toward the development of indolylarylsulfone (IAS) NNRTIs correlated to the carboxamide **1**.[10] Structure−activity relationship (SAR) studies led to the identification of three regions of the IAS scaffold: (region A) the limited spectrum of activity of **1** against mutant HIV-1 strains was significantly expanded by introduction of two methyl groups at positions 3 and 5 of the 3-phenylsulfonyl moiety (**2**);[11] (region B) new potent HIV-1 inhibitors were obtained by coupling the indole-2-carboxamide with either natural or unnatural amino acids; against the mutant L100I, K103N, and Y181C RT HIV-1 strains in CEM cells, IASs **3**−**5** were comparable to efavirenz (EFV);[12,13] (region C) IAS **6** bearing the 5-chloro-4-fluoro substitution pattern at the indole ring was a potent inhibitor of

Received: August 3, 2010
Published: March 02, 2011

Chart 1. Structure of New IASs 12−47 and Reference Compounds 1−11

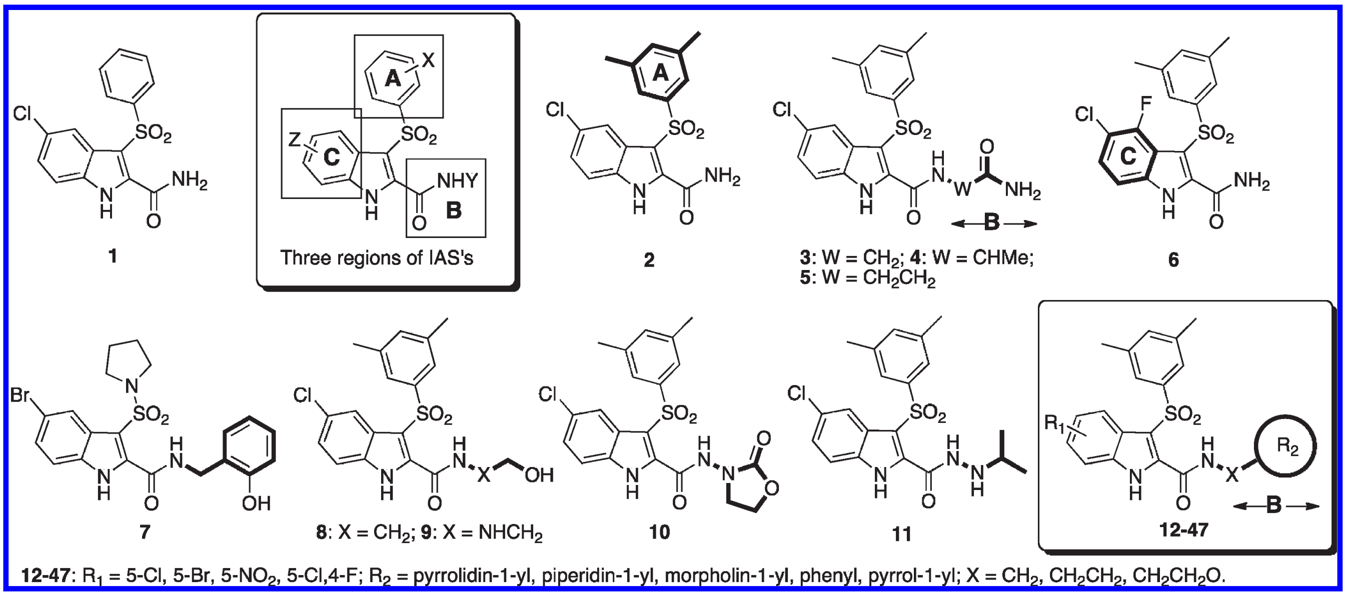

RT WT and RTs carrying the K103N, Y181I, and L100I mutations[14] (Chart 1).

In the design of new NNRTIs, the strategy to add a heterocyclic motif to the parent compound conveniently broadened the spectrum of activity against the mutant strains. For example, Janssen synthesized diaryltriazine (DATA) NNRTIs with very good potency against HIV-1 WT and a panel of HIV-1 mutants by intramolecular cyclization of the thiourea moiety of ITU derivatives.[15] BIRL 355 BS is a new NNRTI in advanced development designed by Boehringer Ingelheim on the dipyridodiazepinone scaffold of nevirapine; the addition of the functionalized side tail provided a NNRTI endowed with potent activity against drug resistant isolates of HIV-1.[16] Merck generated NNRTIs with excellent HIV-1 potency (**7**) by replacing the 3-phenylsulfonyl of **1** with a pyrrolidin-1-ylsulfonyl moiety and introducing an additional heterocycle at position 2 of the indole.[17]

Previously, we synthesized potent IAS derivatives bearing a *N*-(2-hydroxyethyl)carboxamide/carbohydrazide (**8**, **9**) functionality at position 2 of the indole (B region) and two methyl groups at the positions 3 and 5 of the 3-benzenesulfonyl moiety (A region).[18] As further development of that research project, we synthesized new hydrazide derivatives (**10**, **11**) that proved to be more active than EFV against the viral RT carrying the K103N mutation.[19]

Docking studies inside the non-nucleoside binding site (NNBS) of the RT showed that the poses of **8** and **9** (not shown) presented the indole ring rotated by about 180° compared to **2**, while the 3-(3,5-dimethylphenyl) groups overlapped well with the corresponding group of **2** (Figure 1). This new orientation allowed the 2-hydroxyethylamide/hydrazide moieties to fit into the NNBS entrance channel formed by Val106, Pro225, Phe227, Leu234, His235, Pro236, and Tyr318. Furthermore, **8** and **9** established a H-bond between the terminal OH of the ethanolamide/hydrazide chains and the carbonyl group of Leu234.[18] In the case of **11** (not shown), the docking results showed that the isopropyl group occupied a pocket formed by Val106, Pro225, Phe227, Leu234, and Pro236.[19] The latest IASs series reported[13] (compounds **3**−**5**)

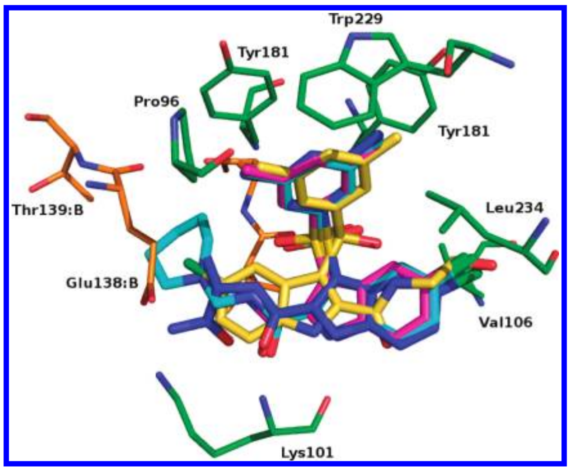

Figure 1. Binding mode of derivatives **2** (magenta), **4** (blue), **8** (yellow), and **16** (cyan). Binding site residues are also reported. Residues of the cleft between the p66 and p51 RT subunits are reported in orange. Val179 (up) and Ile180 (down) are visible behind the docked structures.

showed a different binding mode compared to **8** and **9**. In fact, the putative binding for **3**−**5** was very similar to the one observed for compound **2**. In particular, the side chain at position 2 of the indole nucleus lay in a cleft of the NNBS located at the interface between the p66 (chain A) and p51 (chain B) RT subunits, forming a strong H-bond with Glu138:B (orange residue in Figure 1).[13] Preliminary docking studies showed that new IASs bearing (hetero)cyclic substituents at the indole-2-carboxamide moiety (**16**, Figure 1) could adopt binding poses similar to those of **3**−**5**,[13] establishing novel binding interactions in the solvent accessible cleft of the NNBS described above and in particular formed by residues Arg172, Ile180, Val179 and Glu138:B, and Thr139:B. Starting from these observations, we focused our interest on exploring further the B region of IASs by new substitutions at the indole-2-carboxamide. In particular, our attention was on the introduction of a basic nitrogen atom in the side chain that could interact more

Scheme 1. Synthesis of Compounds 12−23[a]

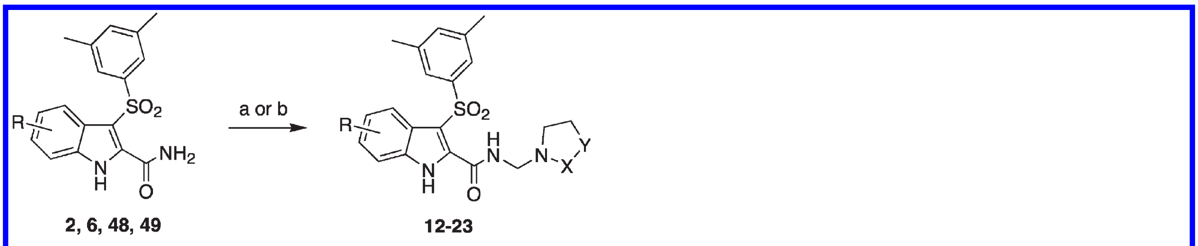

12: R = 5-Cl, X = Y = CH_2; **13**: R = 5-Br, X = Y = CH_2; **14**: R = 5-NO_2, X = Y = CH_2; **15**: 5-Cl,4-F, X = Y = CH_2; **16**: R = 5-Cl, X = CH_2CH_2, Y = CH_2; **17**: R = 5-Br, X = CH_2CH_2, Y = CH_2; **18**: R = 5-NO_2, X = CH_2CH_2, Y = CH_2; **19**: 5-Cl,4-F, X = CH_2CH_2, Y = CH_2; **20**: R = 5-Cl, X = CH_2CH_2, Y = O; **21**: R = 5-Br, X = CH_2CH_2, Y = O; **22**: R = 5-NO_2, X = CH_2CH_2, Y = O; **23**: 5-Cl,4-F, X = CH_2CH_2, Y = O; **2**:[11] R = 5-Cl; **48**:[11] R = 5-Br; **49**: R = 5-NO_2; **6**:[14] R = 5-Cl,4-F.

[a] Reagents and reaction conditions: (a) R = 5-Cl or 5-NO_2, secondary amine, 37% formaldehyde, *t*-BuOH, reflux, 7 h; (b) R = 5-Br or 5-Cl,4-F, secondary amine, paraformaldehyde, benzene, reflux, 3 h, Dean−Stark apparatus.

Scheme 2. Synthesis of Compounds 24−47[a]

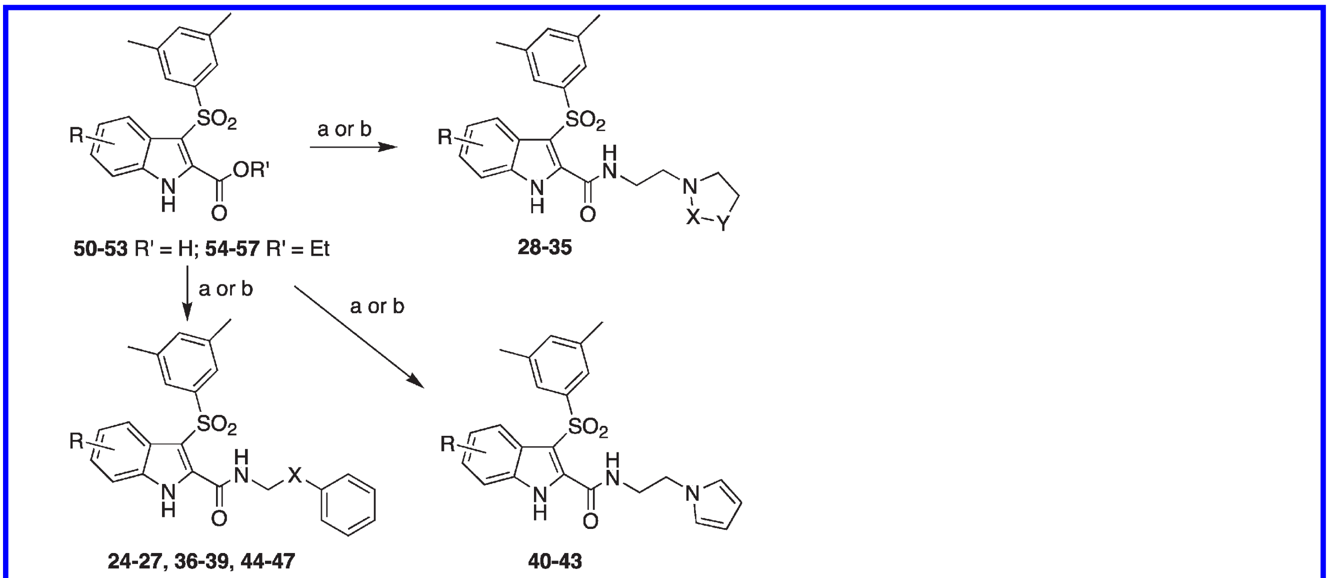

24: R = 5-Cl, X = 0; **25**: R = 5-Br, X 0; **26**: R = 5-NO_2, X = 0; **27**: 5-Cl,4-F, X = 0; **28**: R = 5-Cl, X = Y = CH_2; **29**: R = 5-Br, X = Y = CH_2; **30**: R = 5-NO_2, X = Y = CH_2; **31**: 5-Cl,4-F, X = Y = CH_2; **32**: R = 5-Cl, X = CH_2CH_2, Y = O; **33**: R = 5-Br, X = CH_2CH_2, Y = O; **34**: R = 5-NO_2, X = CH_2CH_2, Y = O; **35**: 5-Cl,4-F, X = CH_2CH_2, Y = O; **36**: R = 5-Cl, X = CH_2; **37**: R = 5-Br, X = CH_2; **38**: R = 5-NO_2, X = CH_2; **39**: 5-Cl,4-F, X = CH_2; **44**: R = 5-Cl, X = CH_2O; **45**: R = 5-Br, X = CH_2O; **46**: R = 5-NO_2, X = CH_2O; **47**: 5-Cl,4-F, X = CH_2; **50**:[13] R = 5-Cl, R' = H; **51**:[13] R = 5-Br, R' = H; **52**:[13] R = 5-NO_2, R' = H; **53**:[13] 5-Cl,4-F, R' = H; **54**:[13] R = 5-Cl, R' = Et; **55**:[13] R = 5-Br, R' = Et; **56**:[13] R = 5-NO_2, R' = Et; **57**:[13] 5-Cl,4-F, R' = Et.

[a] Reagents and reaction conditions: (a) R = 5-Cl, 5-Br, or 5-NO_2, R′ = H, BOP reagent, primary amine, triethylamine, DMF, room temperature, overnight; (b) R = 5-Cl, 5-Cl-4-F, R′ = H, amine, ethanol, closed vessel, 150 °C, 150 W, P_{max} = 250 PSI, ramp time 3 min, hold time 15 min.

efficiently with the Glu138:B acid function and the presence of small hydrophobic groups that could establish nonpolar interactions with the hydrophobic side chains of the residues in the cleft. Furthermore, such a chemical modification could lead to an improvement of the IAS's pharmacokinetic properties.[20,21] We here describe the synthesis and the antiretroviral activity of a new series of IAS compounds (**12**−**47**) characterized by (a) a cycloalkylamino, aryl, or heteroaryl nucleus linked through (b) a methylene, ethylene, or ethoxy linker to the 2-carboxamide and (c) different electron-withdrawing substituents at positions 4 and 5 of the indole (Chart 1).

■ CHEMISTRY

The synthesis of new IASs **12**−**23** is depicted in Scheme 1. Mannich reaction of 5-chloro- (**5**)[11] or 5-nitro-3-[(3,5-dimethylphenyl)sulfonyl]-1*H*-indole-2-carboxamide (**49**) with pyrrolidine, piperidine, or morpholine in *tert*-butanol at reflux temperature for 7 h in the presence of 37% formaldehyde provided the corresponding amines **12**, **14**, **16**, **18**, **20**, and **22**. On the other hand, amines **13**, **15**, **17**, **19**, **21**, and **23** were obtained from 5-bromo- (**48**)[11] or 5-chloro-4-fluoro-3-[(3,5-dimethylphenyl)sulfonyl]-1*H*-indole-2-carboxamide[14] (**6**) and pyrrolidine, piperidine, or morpholine in boiling benzene for 3 h in the

Table 1. Structure and Anti-HIV Activity of New IAS Derivatives 12−27 in CEM Cells[a]

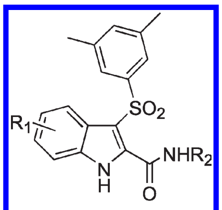

12-27

Compd	R_1	R_2	EC_{50}[b,d] (nM) HIV-1 (III_B)	HIV-2 (ROD)	CC_{50}[c,d] (μM)	SI[e]
12	5-Cl		3.3 ± 3.0	>2000	11 ± 6	3333
13	5-Br		1.3 ± 0.0	>2000	9.6 ± 1.5	7385
14	5-NO_2	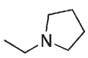	2.5 ± 1.6	7800 ± 1900	12 ± 2	4800
15	5-Cl,4-F		3.9 ± 2.3	>2000	9.3 ± 0.4	2385
16	5-Cl		1.3 ± 0.0	>2000	9.9 ± 0.5	7615
17	5-Br		3.7 ± 1.8	>2000	10 ± 1	2703
18	5-NO_2	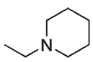	3.1 ± 2.6	7500 ± 2300	12 ± 2	3871
19	5-Cl,4-F		3.9 ± 4.0	>10000	32 ± 2	8205
20	5-Cl		1.9 ± 1.1	>2000	11 ± 3	5789
21	5-Br		3.4 ± 2.2	>10000	35 ± 8	10294
22	5-NO_2	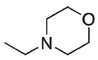	5.8 ± 1.3	≥10000	46 ± 7	7931
23	5-Cl,4-F		2.5 ± 2.3	>10000	38 ± 16	15200
24	5-Cl		5.7 ± 2.1	>10000[f]	244 ± 66	42807
25	5-Br		5.7 ± 1.3	>2000[f]	172 ± 23	30175
26	5-NO_2	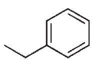	6.2 ± 1.6	>2000[f]	8.0 ± 0.0	1290
27	5-Cl,4-F		5.8 ± 0.42	>2000[f]	15 ± 1	2586
NVP	-	-	19.2 ± 0.0	>10000	>10000	>520
EFV	-	-	1.5 ± 0.3	>10000	>10000	>6667

[a] Data are mean values of two experiments performed in triplicate. [b] EC_{50}: effective concentration (nM) or concentration required to protect CEM cells against the cytopathicity of HIV by 50%, as monitored by giant cell formation. [c] CC_{50}, cytostatic concentration: compound concentration (μM) required to reduce by 50% the number of viable cells in mock-infected CEM cultures. [d] Syncytia cell formation was examined microscopically. [e] Selectivity index was calculated as the ratio CC_{50}/EC_{50}. [f] Compound precipitation was detected at higher compound concentrations.

presence of paraformaldehyde using a Dean−Stark apparatus (Scheme 1).

Reaction in sequence of 5-chloro- (**50**),[13] 5-bromo- (**51**),[13] or 5-nitro-3-[(3,5-dimethylphenyl)sulfonyl]-1*H*-indole-2-carboxylic acid[13] (**52**) with (benzotriazol-1-yloxy)tris(dimethylamino) phosphonium hexafluorophosphate (BOP reagent) and then with benzylamine, 1-(2-aminoethyl)pyrrolidine, 4-(2-aminoethyl)morpholine, 2-aminoethylbenzene, 1-(2-aminoethyl)pyrrole, or 1-(2-aminoethyl-1-oxy)benzene in the presence of triethylamine in DMF at room temperature overnight afforded carboxamides **24**−**26**, **29**, **30**, **32**−**34**, **36**−**38**, **40**−**42**, and **44**−**47**. Carboxamides **27**, **28**, **31**, **35**, **39**, **43**, and **47** were preferably obtained by microwave-assisted (MW) reaction of 5-chloro-4-fluoro-3-[(3,5-dimethylphenyl)sulfonyl]-1*H*-indole-2-carboxylate (**57**)[13] or, in the case of **28**, the corresponding 5-chloro derivative (**54**),[13] with the appropriate amine in ethanol at 150 W for 15 min (Scheme 2).

■ RESULTS AND DISCUSSION

On the basis of our molecular modeling results, we first synthesized Mannich base **16** which was more potent than **4**[13] against mutant L100I and Y181I RT HIV-1 strains[22] and equipotent to **4** against K103N RT HIV-1 (Table 2 and Figure 1). In the enzymatic assay, compound **16** was 1 order of magnitude more potent than EFV against the WT HIV-1 RT and >160 times more potent than EFV against K103N RT, which is the major mutation emerging in patients treated with EFV, whose viral loads rebound after an initial response to the drug.[23] Such results prompted us to synthesize new IASs by replacing the chloro atom at position 5 of the indole with bromo or nitro (in our previous studies, 5-nitro-IASs were less cytostatic than the corresponding monohalogenated counterparts)[13] or with the 5-chloro-4-fluoroindole substitution which was effective for the antiviral activity of carboxamide **6**.[14]

Replacement of the piperidin-1-yl nucleus of **16** with a pyrrolidin-1-yl ring provided IASs **12**−**14** which showed potent antiretroviral activity against the mutant panel of virus strains. On the contrary, replacing of the piperidin-1-yl nucleus with a morpholin-4-yl one (**20**−**22**) resulted in a general drop of the activity against all the RTs. Therefore, we replaced the morpholin-4-yl moiety with the more lipophilic phenyl ring (**24**−**28**). IASs **24** and **26** showed good activity against the mutant L100I RT HIV1 strain, superior to NVP and EFV, but they were less effective against both K103N and Y181I RTs.

IAS derivatives **12**−**47** were evaluated against the HIV-1 WT in human T-lymphocyte (CEM) cells. Against HIV-1 WT, the

Table 2. HIV-1 RT Inhibitory Activity of Compounds 12−27 and Reference Compounds 4, NVP, and EFV against the WT and Mutant Enzymes Carrying Single Amino Acid Substitutions[a]

	IC_{50}[b] (nM)			
compd	WT	L100I	K103N	Y181I
12	12	26	96	442
13	8	14	67	418
14	34	54	287	1023
15	nd[c]	nd[c]	nd[c]	nd[c]
16	8	37	120	581
17	30	19	125	497
18	13	10	307	999
19	nd[c]	nd[c]	nd[c]	nd[c]
20	54	117	512	5481
21	168	100	863	4303
22	150	99	864	1602
23	80	241	1172	10210
24	21	15	>40000	>40000
25	1054	273	1852	>40000
26	17	14	459	>40000
27	40	40	144	>40000
4[d]	23	112	190	2493
NVP[d]	400	9000	7000	>20000
EFV[d]	80	nd[c]	>20000	400

[a] Data represent mean values of at least three separate experiments. [b] Compound concentration (IC_{50}, nM) required to inhibit by 50% the RT activity of the indicated strain. [c] nd: no data. [d] Reference 13.

inhibitory activities (EC_{50} values) of **12**−**27** seemed only marginally affected by the substitutions at the positions 4 and 5 of the indole nucleus, and no correlation between cLogP and biological activity was observed (Table 1S of Supporting Information).[24,25] We previously observed similar results for IASs bearing an amino acid unit at the indole-2-carboxamide.[13] In contrast, a strong influence of the substituents at the positions 4 and 5 on the anti-HIV-1 activity of IASs was observed in the presence of the primary 2-carboxamide functionality.[11,13,14] As expected, the compounds did not inhibit the HIV-2 strain (Table 1).

Compounds **28**−**31** were 1 order of magnitude less active than the corresponding Mannich bases **12**−**15** against HIV-1 WT in CEM cells; a similar behavior was observed against the panel of the mutated RTs (Tables 3 and 4). The drop of antiviral activity of **28**−**31** might be due to the suboptimal length of the methylene linker.

We replaced the pyrrolidin-1-yl nucleus of **28**−**31** with a phenyl ring to give IASs **36**−**39**. Such a chemical modification improved potency against the mutant L100I HIV-1 strain, but the activity against K103N dropped. With the only exception of **33**, *N*-(morpholinyl)ethyl derivatives **32**−**35** were equipotent to the corresponding methylenes **20**−**23** against HIV-1 WT in CEM cells. Against L100I RT, **32**−**35** were comparable to **20**−**23**, but they were less potent against the mutant K103N and Y188I RT strains.

Neither introduction of a phenethoxy linker (**44**−**47**; **44** is the pheneylther of IAS **8**[18]), nor further lengthening of the alkyl chain (data not shown) resulted in effective inhibition of the mutant HIV-1 strains.

On the basis of our know-how in pyrrole bioisosterism,[26] we decided to introduce a pyrrol-1-yl nucleus at position C2 of the linker. Indeed, IASs **40**−**43** potently inhibited HIV-1 WT in CEM cells at nanomolar concentrations. Notably, such compounds were potent inhibitors of the HIV-1 WT RT and the RTs carrying the L100I and K103 mutations, but they failed to inhibit Y181I RT.

Compounds **20**, **24**−**26**, **28**, **36**, **40**, and **44** were evaluated in CEM cells against mutant HIV-1 strains harboring L100I, K103N, Y181C, Y188L, and E138K single amino acid mutations in the RT (Table 5). Compounds **20**, **24**−**26**, **36**, and **40** were potent inhibitors of the mutant L100I and K103N RT HIV-1 strains, and they were comparable to **4** and superior to NVP and EFV. Against these mutant strains, **20**, **24**−**26**, and **40** were equipotent to ETV (data not shown). Compounds **20**, **24**−**26**, and **40** were comparable to EFV against the mutant Y181C RT HIV-1 strain. Three compounds, **20**, **24**, and **26**, were equipotent to EFV against the mutant Y188L RT HIV-1 strain. Finally, **20**, **24**−**26**, **36**, and **40** were comparable to EFV and ETV (data not shown) against the E138K RT HIV-1 mutant. Such results were in agreement with the inhibitory effect observed against the corresponding mutant RT enzymes (Tables 2 and 4). Further information about cytotoxicity, SI, and relative factor (RF) of compounds **20**, **24**−**26**, **28**, **36**, **40**, and **44** against mutant HIV-1 strains is available in Table 2S and Table 3S of Supporting Information.

To ascertain that the test compounds were also inhibitory in primary T-lymphocyte cells using virus strains that belong to different clades of HIV-1, compounds **12**, **40**, and **20** were included in this study (Table 6). The compounds proved to be exquisitely inhibitory against virus members that belonged to clade A, clade B, clade C, clade A/E, and group O (EC_{50} in the higher picomolar or lower nanomolar range). The clade viruses, in contrast to HIV-1(III_B), were R-tropic. The group O virus was X-tropic. These data point to a broad spectrum of anti-HIV-1 activity of this class of compounds.

MOLECULAR MODELING STUDIES

The binding mode of the IASs was extensively studied by means of docking experiments into the RT NNBS. The aim of the docking simulations was to evaluate our hypothesis that targeting the cleft of the NNBS located at the interface between the p66 and p51 subunits could improve the anti-HIV-1 activity of the IASs.

In our previous studies,[13,27] we reported the comparison between four docking software packages (AutoDock3.0,[28] PLANTS1.1,[29] FlexX,[30] and MOE docking algorithm[31]) in term of ability to reproduce the co-crystallized binding pose of the ligand for a training set of seven different crystal structures of the RT (2rf2,[32] 1vrt,[33] 2zd1,[34] 1fk0,[35] 1s1t,[36] 2opq,[37] and 1jkh[38]). Our experiments showed that PLANTS gave the best results.

The docking experiments were carried out on the WT (2rf2, 1vrt, and 2zd1) and mutated RT (1fk0 K103N mutated RT; 1s1t and 2opq L100I mutated RT; 1jkh Y181C mutated RT). Of the best scored poses of the most active compounds docked into the WT RT, it was possible to visualize a series of well-known interactions: (i) the H-bond was formed between the indole NH and the carbonyl oxygen of Lys101; (ii) the halogen atom at position 5 of the indole established steric rather than electrostatic interactions with the hydrophobic pocket formed by Val106 and Leu234; (iii) an intramolecular H-bond between an oxygen of

Table 3. Structure and Anti-HIV Activity of New IAS Derivatives 28−47 in CEM Cells[a]

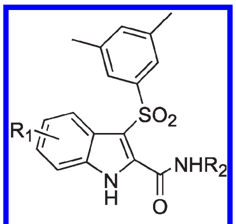

28-47

Compd	R_1	R_2	EC_{50}[b,d] (nM) HIV-1 (III_B)	EC_{50}[b,d] (nM) HIV-2 (ROD)	CC_{50}[c,d] (μM)	SI[e]
28	5-Cl		17 ± 16	>2000	7.1 ± 2.1	418
29	5-Br		16 ± 11	>2000	5.6 ± 3.5	351
30	5-NO_2	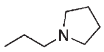	16 ± 11	>10000[f]	21 ± 13	1313
31	5-Cl,4-F		28 ± 0.0	>2000	6.4 ± 0.2	229
32	5-Cl		8.8 ± 4.5	>2000	50 ± 25	5682
33	5-Br		170 ± 21	>50000[f]	409 ± 128	2406
34	5-NO_2	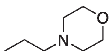	8.0 ± 3.7	4900 ± 570	42 ± 0	5250
35	5-Cl,4-F		13 ± 7.0	≥10000	11 ± 2	846
36	5-Cl		5.7 ± 1.2	>50000	185 ± 5	32456
37	5-Br		14 ± 3.5	>2000[f]	409 ± 128	29214
38	5-NO_2	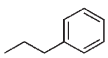	6.8 ± 3.3	>50000[f]	≥500	>72529
39	5-Cl,4-F		14 ± 14	>10000	17 ± 1	1214
40	5-Cl		6.5 ± 2.2	>10000	54 ± 18	8308
41	5-Br		6.4 ± 1.1	>10000[f]	146 ± 40	22813
42	5-NO_2	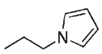	6.9 ± 0.64	≥50000[f]	226 ± 54	32754
43	5-Cl,4-F		5.5 ± 3.2	≥10000	9.8 ± 0.1	1782
44	5-Cl		26 ± 14	>10000[f]	207 ± 23	7962
45	5-Br		29 ± 2.8	>25000	>500	>17241
46	5-NO_2	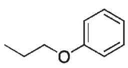	29 ± 13	>2000[f]	>500	>17241
47	5-Cl,4-F		19 ± 9.6	>2000	11 ± 0	549

[a] Data are mean values of two experiments performed in triplicate. [b] EC_{50}: effective concentration (nM) or concentration required to protect CEM cells against the cytopathicity of HIV by 50%, as monitored by giant cell formation. [c] CC_{50}, cytostatic concentration: compound concentration (μM) required to reduce by 50% the number of viable cells in mock-infected CEM cultures. [d] Syncytia cell formation was examined microscopically. [e] Selectivity index was calculated as CC_{50}/EC_{50} ratio. [f] Compound precipitation was detected at higher compound concentrations.

the sulfone group and the amidic nitrogen atom at the side chain stabilized the compound conformation; (iv) the 3,5-dimethylphenyl moiety formed hydrophobic interactions with an aromatic cleft formed by the side chains of Tyr181, Tyr188, Trp229, and Pro96 residues (Figure 1). Our interest was focused on the possibility of enlarging the number of interactions at the p51 and p66 interface cleft.

From analysis of the results for pyrrolidine (**12**) and piperidine (**16**) compounds, it was interesting to observe H-bond/ionic interactions between the nitrogen atom (eventually protonated at physiological condition) of the saturated heterocycle and the Glu138:B carboxylic function. At the same time, the carbon atoms of the heterocycle moiety interacted with Val179 and Ile180 residues inside the cleft and established hydrophobic contacts with the side chains of Glu138:B and Thr139:B (orange residues in Figure 2). The phenyl ring of the derivative **24** could be stabilized only by hydrophobic interactions. In the case of compound **28**, the superior homologue of **12**, the ethylene linker forced the heterocyclic nitrogen distance from Glu138:B carboxylic function from 3 to >4 Å, thus leading to breaking of the H-bond/ionic interaction (Figure 3). No major difference was observed between the binding mode of **36** and its inferior homologue **24** (data not shown).

A series of molecular dynamics simulations were also performed to study the stability of the interactions reported above. In particular, we focused our attention on the reference compound **4** and derivative **12**. For both inhibitors the binding pose was stable during the whole simulation time (rmsd **4**: 1.13 Å; rmsd **12**: 0.98 Å) and the key H-bond with Lys101 had a frequency of formation of 90%, suggesting a high stability. The hydrophobic interactions with Tyr180, Tyr188, and Trp229 were also stable. Some differences were observed in the interaction that compounds **4** and **12** made in the RT p51 and p66 interface cleft. In the case of compound **4** the H-bond between Glu138:B acid function had a rate of formation of 40% and some hydrophobic interactions were established between the methyl groups in the side chain of **4** with Glu138:B and Val179:B. With derivative **12**, the H-bond with Glu138:B was more stable with a higher rate of formation (74%). Furthermore, in addition to the hydrophobic contacts with Glu138:B and Val179:B, a stable nonpolar interaction was engaged with Thr139:B. These results are in accordance with the experimental data and support our rationale.

Table 4. HIV-1 RT Inhibitory Activity of Compounds 28−47 and Reference Compounds 4, NVP, and EFV against the WT and Mutant Enzymes Carrying Single Amino Acid Substitutions[a]

	IC_{50} [b] (nM)			
compd	WT	L1001	K103N	Y181I
28	80	248	660	>40000
29	65	315	697	>40000
30	280	594	1347	>40000
31	158	1547	2405	>40000
32	99	225	6682	>40000
33	63	108	1365	>40000
34	55	421	>40000	>40000
35	711	747	6371	>40000
36	77	27	10390	>40000
37	128	23	1684	>40000
38	60	40	>40000	>40000
39	nd[c]	nd[c]	nd[c]	nd[c]
40	14	34	85	>40000
41	nd[c]	nd[c]	nd[c]	nd[c]
42	34	23	272	>40000
43	18	30	170	3700
44	2395	>40000	>40000	>40000
45	4719	>40000	>40000	>40000
46	950	>40000	>40000	>40000
47	66	68	18500	>40000
4[d]	23	112	190	2493
NVP[d]	400	9000	7000	>20000
EFV[d]	80	nd[c]	>20000	400

[a] Data represent mean values of at least three separate experiments. [b] Compound concentration (IC_{50}, nM) required to inhibit by 50% the RT activity of the indicated strain. [c] nd: no data. [d] Reference 13.

The IASs binding mode was extensively studied in the mutated RTs. The mutation of Leu100 to Ile seemed not to affect the binding mode of IASs **12**−**43**, and all the favorable interactions observed for the WT RT were still detectable for the L100I mutation, as it was confirmed by the small difference between L100I and WT IC_{50} experimental values: **12**, IC_{50} WT = 12 nM and IC_{50} L100I = 26 nM (Figure 1S, Supporting Information).

In the interaction of **12** with the K103N mutated RT, all binding interactions were retained with the only exception of the favorable hydrophobic interaction between the indole core and the carbon atoms of the Lys103 side chain (**12**, IC_{50} K103N = 96 nM) (Figure 2S, Supporting Information).

In the case of the mutation of Tyr181 to Cys, the favorable $\pi-\pi$ interaction between the 3-(3,5-dimethylphenyl) moiety and the phenyl ring of tyrosine completely disappeared. The analysis was in accordance with the biological data justifying the weak anti-HIV-1 activity (**12**, IC_{50} Y181C = 442 nM). Of particular note, from the docking studies no H-bond between the carbonyl oxygen of Glu138:B and the nitrogen atom of the saturated heterocyclic ring of IAS was observed for K103N and Y181C mutations.

■ CONCLUSIONS

We synthesized new IAS derivatives bearing cyclic substituents at the indole-2-carboxamide linked through a methylene/ethylene spacer. Regardless of the length of the spacer group, the new IASs were potent inhibitors of HIV-1 WT replication in CEM cells and showed inhibitory concentrations in the low nanomolar range. The substituents introduced at positions 4 and 5 of the indole did not show a significant effect on the antiviral activity against the HIV-1 WT. 5-Bromo and 5-nitro-IASs bearing the ethylene linker were less cytostatic than the corresponding 5-chloro and 5-chloro-4-fluoro derivatives. Against the mutant L100I and K103N RT HIV-1 strains, compounds **20**, **24**−**26**, **36**, and **40** showed antiviral potency superior to that of NVP and EFV and were comparable to IAS **4**.[13] Against these mutant strains, derivatives **20**, **24**−**26**, and **40** were equipotent to ETV. Compounds **12**, **40**, and **20** proved to inhibit effectively different HIV clades in PBMC with EC_{50} values in the higher picomolar or lower nanomolar range of concentrations. These IASs may be useful in EFV-based HIV-1 therapies that show the emergence of the L100I and K103N mutations. Molecular docking experiments on this novel series of IAS analogues have also suggested that the H-bond interaction between the nitrogen atom in the carboxamide chain of IAS and Glu138:B is important in the binding of these compounds. These results are in accordance with the experimental data obtained on the WT and on the mutant strains tested. These compounds are the first IASs bearing a third cyclic moiety, which may be considered as hydrids between two-wings and horseshoe-conformation NNRTIs.[27] Such results provide useful information for our research project looking at an active conformation for future HIV-1 NNRTIs.

Table 5. Anti-HIV-1 Activity of Compounds 20, 24−26, 28, 36, 40, and 44 and Reference Compounds NVP and EFV against Mutant HIV-1 Strains in MT-4 Cell Cultures[a]

	EC_{50} [a] (nM)					
compd	IIIB	L100I	K103N	Y181C	Y188L	E138K
20	3.2 ± 0.8	8.0 ± 5.6	11 ± 3	23 ± 6	440 ± 60	14 ± 0
24	11 ± 7	6.1 ± 2.4	11 ± 0	46 ± 11	480 ± 90	18 ± 5
25	16 ± 3	11 ± 8	15 ± 3	59 ± 37	≥450	51 ± 41
26	10 ± 7	7 ± 5.1	11 ± 5	54 ± 30	470 ± 200	16 ± 0
28	19 ± 1	84 ± 8	80 ± 5	380 ± 20	>1000	260 ± 100
36	21 ± 3	19 ± 1	52 ± 6	100 ± 10	>1000	65 ± 3
40	15 ± 1	11 ± 1	15 ± 0	67 ± 22	>1000	18 ± 1
44	300 ± 140	440 ± 200	>1000	>1000	>1000	380 ± 20
4	1.6 ± 1.3	9 ± 7	14 ± 6	96 ± 34	660 ± 480	nd[c]
NVP	23 ± 4	60 ± 4	>1000	>1000	>1000	150 ± 75
EFV[b]	1.9 ± 0.3	22 ± 14	130 ± 180	160 ± 180	760 ± 630	9.5 ± 0.3

[a] Data represent the average values ± SD of two to three independent experiments. The cytopathicity assay was based on cell viability measurements determined by the MTT method. The EC_{50} represents the compound concentration required to reduce cell viability by 50%. [b] The determinations of EFV showed a high degree of variability. [c] nd: no data.

■ EXPERIMENTAL SECTION

Chemistry. MW-assisted reactions were performed on a Discover S-Class (CEM) single mode reactor, controlling instrument parameters with PC-running Synergy 1.4 software. Temperature, irradiation power, maximum pressure (Pmax), PowerMAX (*in situ* cooling during the MW irradiation), ramp and hold times, and open and closed vessel modes were set as indicated. Reactions in an open vessel were carried out in 100 mL round-bottom flasks equipped with a Dimroth reflux condenser and

Table 6. Inhibitory Activity of Compounds 12, 20, and 40 against Different HIV-1 Clades in Peripheral Blood Mononuclear Cells (PBMC)

	EC_{50} [a] (nM)				
compd	clade A (UG273)	clade B (BaL)	clade C (DJ259)	clade A/E (ID12)	group O (BCF06)
12	0.1	0.1	0.1	0.3	0.2
20	0.1	0.1	0.5	0.3	0.9
40	2.1	2.3	3.5	2.9	3.2

[a] EC_{50}: 50% effective concentration or compound concentration required to inhibit HIV-1 p24 production in virus-infected PBMC. Data are the mean of two independent experiments.

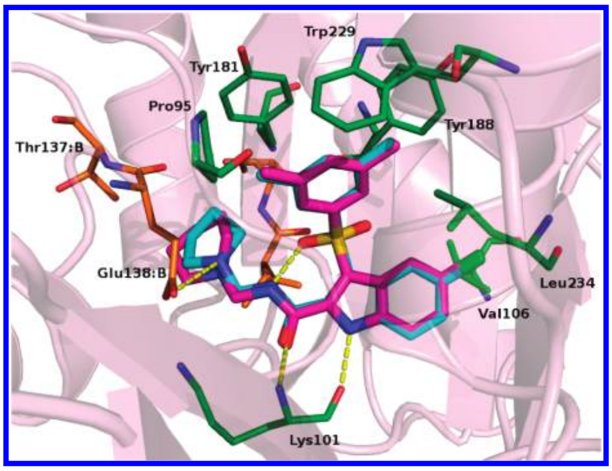

Figure 2. Binding conformation of **12** (cyan) and **16** (magenta) into the NNBS of HIV-1 WT RT. Hydrogen atoms are not shown for clarity. H-Bonds are reported as dotted yellow lines.

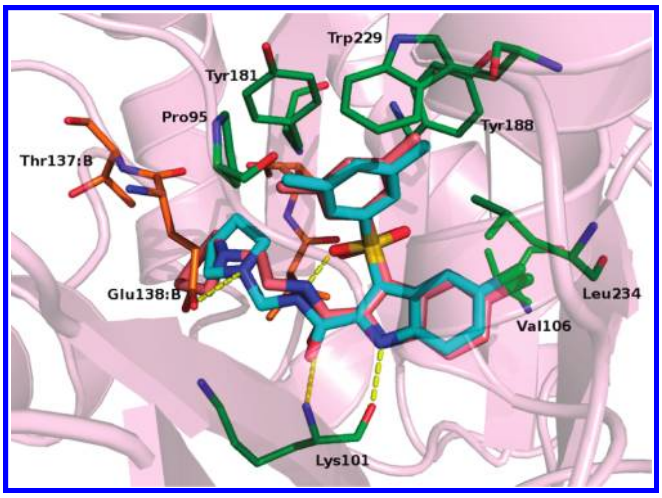

Figure 3. Binding conformation of **12** (cyan) and **28** (pink) into the NNBS of HIV-1 WT RT. Hydrogen atoms are not shown for clarity. H-Bonds are reported as dotted yellow lines.

a cylindrical stirring bar (length 20 mm, diameter 6 mm). Reactions in a closed vessel were performed in capped MW-dedicated vials (10 or 35 mL) with cylindrical stirring bar (length 8 mm, diameter 3 mm). The temperature of the reaction was monitored by a built-in infrared (IR) sensor. After completion of the reaction, the mixture was cooled to 25 °C via air-jet cooling. Melting points (mp) were determined on a SMP1 apparatus (Stuart Scientific) and are uncorrected. IR spectra were run on a SpectrumOne FT-ATR spectrophotometer (Perkin Elmer). Band position and absorption ranges are given in cm^{-1}. Proton nuclear magnetic resonance (^1H NMR) spectra were recorded on a 400 MHz FT spectrometer (Bruker) in the indicated solvent. Chemical shifts are expressed in δ units (ppm) from tetramethylsilane. Column chromatography was performed on columns packed with alumina from Merck (70−230 mesh) or silica gel from Macherey-Nagel (70−230 mesh). Aluminium oxide thin layer chromatography (TLC) cards from Fluka (aluminium oxide precoated aluminium cards with fluorescent indicator visualizable at 254 nm) and silica gel TLC cards from Macherey-Nagel (silica gel precoated aluminum cards with fluorescent indicator visualizable at 254 nm) were used for TLC. Developed plates were visualized by a Spectroline ENF 260C/FE UV apparatus. Organic solutions were dried over anhydrous sodium sulfate. Evaporation of the solvents was carried out on a Büchi Rotavapor R-210 equipped with a Büchi V-850 vacuum controller and Büchi V-700 (∼5 mbar) and V-710 (∼2 mbar) vacuum pumps. Elemental analyses of tested compounds were found within ±0.4% of the theoretical values. Purity of tested compounds was >95%. 5-Chloro-3-[(3,5-dimethylphenyl)sulfonyl]-1*H*-indole-2-carboxamide (**2**),[11] 5-chloro-3-[(3,5-dimethylphenyl)sulfonyl]-4-fluoro-1*H*-indole-2-carboxamide (**6**),[14] 5-bromo-3-[(3,5dimethylphenyl)sulfonyl]-1*H*-indole-2-carboxamide (**48**),[11] 5-chloro-3-[(3,5dimethylphenyl)sulfonyl]-1*H*-indole-2-carboxylic acid (**50**),[13] 5-bromo3-[(3,5dimethylphenyl)sulfonyl]-1*H*-indole-2-carboxylic acid (**51**),[13] 3-[(3,5dimethylphenyl)sulfonyl]-5-nitro-1*H*-indole-2-carboxylic acid (**52**),[13] 5-chloro-3-[(3,5-dimethylphenyl)sulfonyl]-4fluoro-1*H*-indole2-carboxylic acid (**53**),[13] ethyl 5-chloro-3-[(3,5dimethylphenyl)sulfonyl]-1*H*-indole-2-carboxylate (**54**),[13] ethyl 5-bromo3-[(3,5dimethylphenyl)sulfonyl]-1*H*-indole2-carboxylate (**55**),[13] ethyl 3-[(3,5-dimethylphenyl)sulfonyl]-5-nitro-1*H*-indole-2-carboxylate (**56**),[13] and ethyl 5-chloro-3-[(3,5-dimethylphenyl)sulfonyl]-1*H*-indole-2-carboxylate (**57**)[13] were prepared as previously reported.

General Procedure for the Preparation of Derivatives 12, 14, 16, 18, 20, and 22. Example: 5-Chloro-3-[(3,5-dimethylphenyl)sulfonyl]-*N*-(pyrrolidin-1-ylmethyl)-1*H*-indole-2-carboxamide (12). A mixture of **2** (0.43 g, 0.00119 mol) in *tert*-butanol (20 mL) was heated at 100 °C, and pyrrolidine (0.093 g, 0.1 mL, 0.00131 mol) and 37% formaldehyde (0.039 g, 0.1 mL, 0.00131 mol) were added. After 4 h, pyrrolidine (0.093 g, 0.1 mL, 0.00131 mol) and 37% formaldehyde (0.039 g, 0.1 mL, 0.00131 mol) were further added, and the reaction mixture was stirred at the same temperature for additional 3 h. After cooling, *n*-hexane (5 mL) was added and the precipitate collected to give **12** (0.07 g, 13%) as white solid, mp 193-196 °C. ^1H NMR (DMSO-d_6): δ 1.66−1.69 (m, 4H), 2.30 (s, 6H), 2.63−2.66 (m, 4H), 4.32 (d, J = 5.7 Hz, 2H), 7.25 (s, 1H), 7.32 (dd, J = 6.6 and 2.1 Hz, 1H), 7.52 (d, J = 8.7 Hz, 1H), 7.61 (d, J = 8.9 Hz, 2H), 7.91 (d, J = 2.2 Hz, 1H), 9.22 (br s, 1H, disappeared on treatment with D_2O), 13.01 ppm (br s, 1H, disappeared on treatment with D_2O). IR: ν 1678, 3120 cm^{-1}. Anal. ($C_{22}H_{24}ClN_3O_3S$ (445.96)) C, H, Cl, N, S.

Preparative and spectroscopic data of derivatives **14**, **16**, **18**, **20** and **22** are reported in Supporting Information.

General Procedure for the Preparation of Derivatives 13, 15, 17, 19, 21, and 23. Example: 5-Bromo-3-[(3,5-dimethylphenyl)sulfonyl]-*N*-(pyrrolidin-1-ylmethyl)-1*H*-indole-2-carboxamide (13). A mixture of **48** (0.1 g, 0.000 24 mol), paraformaldehyde (0.072 g, 0.000 24 mol), and pyrrolidine (0.017 g, 0.02 mL, 0.000 24 mol) in benzene (15 mL) was refluxed for 3 h using a Dean–Stark apparatus. After cooling, the precipitate was collected and washed with benzene to give **13** (0.07 g, 60%) as white solid, mp 183–186 °C. ^{1}H NMR (DMSO-d_6): δ 1.66–1.70 (m, 4H), 2.29 (s, 6H), 2.63–2.67 (m, 4H), 4.32 (d, J = 4.2 Hz, 2H), 7.26 (s, 1H), 7.41–7.49 (m, 2H), 7.71 (s, 2H), 8.07 (d, J = 1.1 Hz, 1H), 9.21 (br s, 1H, disappeared on treatment with D_2O), 13.01 ppm (br s, 1H, disappeared on treatment with D_2O). IR: ν 1646, 3217 cm^{-1}. Anal. ($C_{22}H_{24}BrN_3O_3S$ (490.41)) C, H, Br, N, S.

Preparative and spectroscopic data of derivatives **15**, **17**, **19**, **21**, and **23** are reported in Supporting Information.

General Procedure for the Preparation of Derivatives 24–26, 29, 30, 32–34, 36–38, 40–42, and 44–46. Example: *N*-Benzyl-5-chloro-3-[(3,5-dimethylphenyl)sulfonyl]-1*H*-indole-2-carboxamide (24). BOP (0.28 g, 0.0016 mol) was added to a mixture of **50** (0.5 g, 0.0014 mol), benzylamine (0.30 g, 0.03 mL, 0.0028 mol), and triethylamine (0.42 g, 0.58 mL, 0.0042 mol) in DMF (28 mL). The reaction mixture was stirred at room temperature overnight, diluted with water and extracted with ethyl acetate. The organic layer was washed with brine, dried, and filtered. Removal of the solvent gave a residue that was purified by column chromatography (silica gel, ethyl acetate as eluent) to give **24** (0.27 g, 43%) as yellow solid, mp 259–262 °C (from ethanol). ^{1}H NMR ($CDCl_3$): δ 2.26 (s, 6H), 4.80 (d, J = 2.9 Hz, 2H), 7.15 (s, 1H), 7025–7.27 (m, 2H), 7.35–7.50 (m, 7H), 8.24–8.25 (m, 1H), 10.17 (br s, 1H, disappeared on treatment with D_2O), 11.25 ppm (br s, 1H, disappeared on treatment with D_2O). IR: ν 1638, 3209 cm^{-1}. Anal. ($C_{24}H_{21}ClN_2O_3S$ (452.95)) C, H, Cl, N, S.

Preparative and spectroscopic data for derivatives **25**, **26**, **29**, **30**, **32–34**, **36–38**, **40–42**, and **44–46** are reported in Supporting Information.

General Procedure for the Preparation of Derivatives 27, 28, 31, 35, 39, 43, and 47. Example: *N*-Benzyl-5-chloro-3-[(3,5-dimethylphenyl)sulfonyl]-4-fluoro-1*H*-indole-2-carboxamide (27). A mixture of **57** (0.1 g, 0.00024 mol) and benzylamine (0.078 g, 0.2 mL, 0.00073 mol) in ethanol (0.15 mL) was placed into the MW cavity (closed vessel mode, P_{max} = 250 PSI). MW irradiation of 150 W was used, the temperature being ramped from 25 °C to 150 °C, while stirring. Once 150 °C was reached, taking about 3 min, the reaction mixture was held there for 15 min. The precipitate was collected and recrystallized from ethanol to give **27** (0.084 g, 75%) as white solid, mp 229-231 °C. ^{1}H NMR (DMSO-d_6): δ 2.30 (s, 6H), 4.56 (d, J = 5.7 Hz, 2H), 7.25 (s, 1H), 7.28 (t, J = 7.2 Hz, 1H), 7.32–7.39 (m, 4H), 7.48 (d, J = 7.1 Hz, 2H), 7.67 (s, 2H), 9.50 (br s, 1H, disappeared on treatment with D_2O), 13.29 ppm (br s, 1H, disappeared on treatment with D_2O). IR: ν 1638, 3220 cm^{-1}. Anal. ($C_{17}H_{15}N_3O_5S$ (470.94)) C, H, Cl, F, N, S.

Preparative and spectroscopic data of derivatives **28**, **31**, **35**, **39**, **43**, and **47** are reported in Supporting Information.

3-[(3,5-Dimethylphenyl)sulfonyl]-5-nitro-1*H*-indole-2-carboxamide (49). A mixture of ethyl 3-[(3,5-dimethylphenyl) sulfonyl]-5-nitro-1*H*-indole-2-carboxylate[13] (0.56 g, 0.0014 mol) was heated with 30% ammonium hydroxide (25 mL) and ammonium chloride (40 mg) in a sealed tube at 100 °C overnight. After cooling, the reaction mixture was poured on ice–water, stirred for 15 min, and extracted with ethyl acetate. The organic layer was washed with brine, dried, and filtered. Removal of the solvent gave a residue that was purified by column chromatography (silica gel, chloroform:ethanol = 95:5) to furnish **49** as white solid (0.31 g, 60%) mp >300 °C (from ethanol). ^{1}H NMR (DMSO-d_6): δ 2.33 (s, 6H), 7.31 (s, 1H), 7.68–7.75 (m, 3H), 8.16–8.24 (m, 1H), 8.34 (br s, disappeared on treatment with D_2O, 1H), 8.50 (br s, disappeared on treatment with D_2O, 1H), 8.87–8.89 (m, 1H), 13.47 ppm (br s, disappeared on treatment with D_2O, 1H). IR (Nujol): ν 1653, 3235, 3310 cm^{-1}. Anal. ($C_{17}H_{15}N_3O_5S$ (373.39)) C, H, N, S.

Molecular Modeling. All molecular modeling studies were performed on a MacPro dual 2.66 GHz Xeon running Ubuntu 9.10. The RT structures were downloaded from the PDB (http://www.rcsb.org/). Hydrogen atoms were added to the protein, using Molecular Operating Environment (MOE) 2007.09[31] and minimized, keeping all the heavy atoms fixed until a rmsd gradient of 0.05 kcal mol^{-1} Å^{-1} was reached. Ligand structures were built with MOE and minimized using the MMFF94x force field until a rmsd gradient of 0.05 kcal mol^{-1} Å^{-1} was reached. The docking simulations were performed using PLANTS.[29] We set the binding lattice as a sphere of 12 Å binding site radius from the center of 2rf2[32] co-crystallized inhibitor. Also, in this case we used all default settings. The Y181I mutation was obtained by mutating the specific residue in the 1jkh[38] crystal using the rotamer explorer tool in MOE and using the lowest energy conformation obtained. The calculation of the rmsd values between the cocrystallized and docked conformation were calculated by the MOE SVL script.[39]

Molecular dynamics was performed with the AMBER 9 suite.[40,41] The minimized structure was solvated in a periodic octahedron simulation box using TIP3P water molecules, providing a minimum of 10 Å of water between the protein surface and any periodic box edge. Chlorine ions were added to neutralize the charge of the total system. The water molecules and chlorine ions were energy-minimized keeping the coordinates of the protein–ligand complex fixed (1000 cycle), and then the whole system was minimized (5000 cycle). Following minimization, the entire system was heated to 298 K (5 ps). The production simulation was conducted at 298 K with constant pressure and periodic boundary condition. Shake bond length condition was used (ntc = 2). Compounds were parametrized by Antechamber[42,43] using AM1 charges. Trajectories analysis were carried our by ptraj[44] program. The images in the manuscript were created with PyMOL.[45]

Inhibition of HIV-Induced Cytopathicity. The methodology for the anti-HIV assays had been described previously.[46] Briefly, human CEM cell cultures (~3 × 10^5 cells mL^{-1}) were infected with ~100 $CCID_{50}$ HIV-1(IIIB) or HIV-2 (ROD) per mL and seeded in 200 μL well microtiter plates, containing appropriate dilutions of the test compounds. After 4 days of incubation at 37 °C, syncytia cell formation was examined microscopically in the CEM cell cultures.

The anti-HIV activity of several compounds against wild-type HIV-1 strain IIIB and a variety of RT mutant HIV-1 strains in MT-4 cell cultures was determined using the 3-(4,5-dimethylthiazol-2-yl)-2,5-diphenyltetrazolium bromide (MTT) method.[47] Briefly, virus stocks were titrated in MT-4 cells and expressed as the 50% cell culture infective dose ($CCID_{50}$). MT-4 cells were suspended in culture medium at 1 × 10^5 cells/mL and infected with HIV at a multiplicity of infection of 0.02. Immediately after viral infection, 100 μL of the cell suspension was placed in each well of a flat-bottomed microtiter tray containing various concentrations of the test compounds. The test compounds were dissolved in DMSO at 50 mM or higher. After 4 days of incubation at 37 °C, the number of viable cells was determined using the MTT method. The selection and characterization of mutant virus strains have been performed previously.

Inhibition of Different HIV-1 Clades in PBMC. PBMC from healthy donors were isolated by density gradient centrifugation and stimulated with PHA at 2 μg/mL (Sigma) for 3 days at 37 °C. The PHA-stimulated blasts were washed twice with phosphate-buffered saline and counted by trypan blue. The cells were then seeded at 0.5 × 10^6 cells per well into a 48-well plate containing varying concentrations of compound in cell culture medium (RPMI 1640) containing 10% fetal calf serum and interleukin-2 (25 units/mL, R&D Systems Europe, Abingdon, U.K.). The virus stocks were diluted in medium and added at a final dose of 250 pg of p24/mL as determined by a viral core antigen (Ag) specific enzyme-linked immunosorbent assay. Cell supernatant was collected at days 10–12, and HIV-1 core Ag in the culture supernatant was analyzed by a p24 Ag enzyme-linked immunosorbent assay kit (PerkinElmer Life Sciences).

Cytostatic Assays. The cytostatic concentration was calculated as the CC_{50}, the compound concentration required to reduce CEM cell proliferation by 50% relative to the number of cells in the untreated controls. CC_{50} values were estimated from graphic plots of the number of cells determined by Coulter counter measurements (percentage of control) as a function of the concentration of the test compounds.

Enzymatic Assay Procedures. Chemicals. [^{3}H]dTTP (40 Ci/mmol) was from Amersham, and unlabeled dNTPs were from Boehringer. Whatman was the supplier of the GF/C filters. All other reagents were of analytical grade and purchased from Merck or Fluka.

Nucleic Acid Substrates. The homopolymer poly(rA) (Pharmacia) was mixed at weight ratios in nucleotides of 10:1 with the oligomer oligo$(dT)_{12-18}$ (Pharmacia) in 20 mM Tris-HCl (pH = 8.0), containing 20 mM KCl and 1 mM EDTA, heated at 65 °C for 5 min, and then slowly cooled at room temperature.

Expression and Purification of Recombinant HIV-1 RT Forms. The coexpression vectors pUC12N/p66(His)/p51with the WT or the mutant forms of HIV-1 RT p66 were kindly provided by Dr. S. H. Hughes (NCI-Frederick Cancer Research and Development Center). Proteins were expressed in *E. Coli* and purified as described.[48]

HIV-1 RT RNA-Dependent DNA Polymerase Activity Assay. RNA-dependent DNA polymerase activity was assayed as follows: a final volume of 25 μL contained reaction buffer (50 mM Tris-HCl pH 7.5, 1 mM DTT, 0.2 mg/mL BSA, 4% glycerol), 10 mM $MgCl_2$, 0.5 μg of poly(rA)/oligo$(dT)_{10:1}$ (0.3 μM 3′-OH ends), 10 μM [^{3}H]dTTP (1 Ci/mmol), and 2−4 nM RT. Mixtures were incubated at 37 °C for the indicated time. Then 20 μL aliquots were spotted on glass fiber filters GF/C which were immediately immersed in 5% ice-cold TCA. Filters were washed twice in 5% ice-cold TCA and once in ethanol for 5 min, dried and acid-precipitable radioactivity was quantitated by scintillation counting.

Inhibition Assay. Reactions were performed under the conditions described for the HIV-1 RT RNA-dependent DNA polymerase activity assay. Incorporation of radioactive dTTP into poly(rA)/oligo(dT) at different substrate (nucleic acid or dTTP) concentrations was monitored in the presence of increasing fixed amounts of inhibitor. Data were then plotted according to Lineweaver−Burke and Dixon. For K_i determination, an interval of inhibitor concentrations between $0.2K_i$ and $5K_i$ was used.

ASSOCIATED CONTENT

Supporting Information. Additional synthesis and characterization information. This material is available free of charge via the Internet at http://pubs.acs.org.

AUTHOR INFORMATION

Corresponding Author

*Phone: +39 06 4991 3800. Fax: +39 06 4969 3268. E-mail: romano.silvestri@uniroma1.it.

ACKNOWLEDGMENT

The authors are indebted to Istituto Pasteur, Fondazione Cenci Bolognetti (Grant 2009) and FILAS (Finanziaria Laziale di Sviluppo, Grant 2010) for financial support. The authors also thank I. Nikolova and A. Galabov, Bulgarian Academy of Sciences, Sofia, Bulgaria, for the biological evaluation against Coxsackie B4 virus.

ABBREVIATIONS USED

IAS, indolylarylsulfone; HIV-1, human immunodeficiency virus type 1; AIDS, acquired immunodeficiency syndrome; RT, reverse transcriptase; NRTI, nucleoside reverse transcriptase inhibitor; NNRTI, non-nucleoside reverse transcriptase inhibitor; HAART, highly active antiretroviral therapy; WT, wilde type; NVP, nevirapine; EFV, efavirenz; ETV, etravirine; CEM cells, human T-lymphocyte cells

REFERENCES

(1) (a) Barre-Sinoussi, F.; Chermann, J.; Rey, F.; Nugeyre, M.; Chamaret, S.; Gruest, J.; Dauguet, C.; Axler-Blin, C.; Vezinet-Brun, F.; Rouzioux, C.; Rozenbaum, W.; Montagnier, L. Isolation of a T-lymphotric retrovirus from a patient for a risk of acquired immunodeficiency syndrome (AIDS). *Science* **1983**, *220*, 868–871. (b) Gallo, R. C.; Sarin, P. S.; Gelmann, E. P.; Robert-Guroff, M.; Richardson, E.; Kalyanaraman, V. S.; Mann, D.; Sidhu, G. D.; Stahl, R. E.; Zolla.Pazner, S.; Leibowitch, J.; Popovic, M. Isolation of human T-cell leukemia virus in acquired immunodeficiency syndrome (AIDS). *Science* **1983**, *220*, 865–867.

(2) 2009 AIDS epidemic update.

(3) (a) Mehellou, Y.; De Clercq, E. Twenty-six years of anti-HIV drug discovery: where do we stand and where do we go? *J. Med. Chem.* **2010**, *53*, 521–538. (b) De Clercq, E. Highlights in the discovery of antiviral drugs: a personal retrospective. *J. Med. Chem.* **2010**, *53*, 1438–1450.

(4) Este, J. A.; Cihlar, T. Current status and challenges of antiretroviral research and therapy. *Antiviral Res.* **2010**, *85*, 25–33.

(5) (a) Menéndez-Arias, L. Molecular basis of human immunodeficiency virus drug resistance: an update. *Antiviral Res.* **2010**, *85*, 210–231. (b) Paredes, R.; Clotet, B. Clinical management of HIV-1 resistance. *Antiviral Res.* **2010**, *85*, 245–265.

(6) Hawkins, T. Understanding and managing the adverse effects of antiretroviral therapy. *Antiviral Res.* **2010**, *85*, 201–209.

(7) Ceccherini-Silberstein, F.; Svicher, V.; Sing, T.; Artese, A.; Santoro, M. M.; Forbici, F.; Bertoli, A.; Alcaro, S.; Palamara, G.; d'Arminio Monforte, A.; Balzarini, J.; Antinori, A.; Lengauer, T.; Perno, C. F. Characterization and structural analysis of novel mutations in human immunodeficiency virus type 1 reverse transcriptase involved in the regulation of resistance to nonnucleoside inhibitors. *J. Virol.* **2007**, *81*, 11507–11519.

(8) Sweeney1, Z. K.; Klumpp, K. Improving non-nucleoside reverse transcriptase inhibitors for first-line treatment of HIV infection: the development pipeline and recent clinical data. *Curr. Opin. Drug Discovery Dev.* **2008**, *11*, 454–470.

(9) (a) Vingerhoets, J.; Azijn, H.; Fransen, E.; De Baere, I.; Smeulders, L.; Jochmans, D.; Andries, K.; Pauwels, R.; de Bethune, M.-P. TMC125 displays a high genetic barrier to the development of resistance: evidence from in vitro selection experiments. *J. Virol.* **2005**, *79*, 12773–12782. (b) Haubrich, R.; Gubernick, S.; Yasothan, U.; Kirkpatrick, P. Etravirine. *Nat. Rev. Drug Discovery* **2008**, *7*, 287–288.

(10) (a) Williams, T. A.; Ciccarone, T. M.; Saari, W. S.; Wai, J. S.; Greenlee, W. J.; Balani, S. K., Goldman, M. E.; Theoharides, A. D. Indoles as Inhibitors of HIV Reverse Transcriptase. *Eur. Pat. Appl.* EP 0 530 907 A1, 1992. (b) Williams, T. M.; Ciccarone, T. M.; MacTough, S. C.; Rooney, C. S.; Balani, S. K.; Condra, J. H.; Emini, E. A.; Goldman, M. E.; Greenlee, W. J.; Kauffman, L. R.; O'Brien, J. A.; Sardana, V. V.; Schleif, W. A.; Theoharides, A. D.; Anderson, P. S. 5-Chloro-3-(phenylsulfonyl)indole-2-carboxyamide: a novel non-nucleoside inhibitor of the HIV-1 reverse transcriptase. *J. Med. Chem.* **1993**, *36*, 1291–1294.

(11) Silvestri, R.; De Martino, G.; La Regina, G.; Artico, M.; Massa, S.; Vargiu, L.; Mura, M.; Loi, A. G.; Marceddu, T.; La Colla, P. Novel indolyl aryl sulfones active against HIV-1 carrying NNRTI resistance mutations: synthesis and SAR studies. *J. Med. Chem.* **2003**, *46*, 2482–2493.

(12) Silvestri, R.; Artico, M.; De Martino, G.; La Regina, G.; Loddo, R.; La Colla, M.; La Colla, P. Simple, short peptide derivatives of a sulfonylindolecarboxamide (L-737,126) active in vitro against HIV-1 wild-type and variants carrying non-nucleoside reverse transcriptase inhibitor resistance mutations. *J. Med. Chem.* **2004**, *47*, 3892–3896.

(13) Piscitelli, F.; Coluccia, A.; Brancale, A.; La Regina, G.; Sansone, A.; Giordano, C.; Balzarini, J.; Maga, G.; Zanoli, S.; Samuele, A.; Cirilli, R.; La Torre, F.; Lavecchia, A.; Novellino, E.; Silvestri, R. Indolylarylsulfones bearing natural and unnatural amino acids. Discovery of potent inhibitors of HIV-1 non-nucleoside wild type and resistant mutant strains reverse transcriptase and coxsackie B4 virus. *J. Med. Chem.* **2009**, *52*, 1922–1934.

(14) La Regina, G.; Coluccia, A.; Piscitelli, F.; Bergamini, A.; Sinistro, A.; Cavazza, A.; Maga, G.; Samuele, A.; Zanoli, S.; Novellino, E.; Artico, M.; Silvestri, R. Indolyl aryl sulfones as HIV-1 non-nucleoside reverse transcriptase inhibitors: role of two halogen atoms at the indole ring in developing new analogues with improved antiviral activity. *J. Med. Chem.* **2007**, *50*, 5034–5038.

(15) Ludovici, D. W.; Kavash, R. W.; Kukla, M. J.; Ho, C. Y.; Ye, H.; De Corte, B L.; Andries, K.; de Béthune, M.-P.; Azijn, H.; Pauwels, R.; Moereels, H. E. L.; Heeres, J.; Koymans, L. M. H.; de Jonge, M. R.; Van Aken, K. J. A.; Daeyaert, F. F. D.; Lewi, P. J.; Das, K.; Arnold, E.; Janssen, P. A. J. Evolution of anti-HIV drug candidates part 2: diaryltriazine (DATA) analogues. *Bioorg. Med. Chem. Lett.* **2001**, *11*, 2229–2234.

(16) (a) Klunder, J. M.; Hoermann, M.; Cywin, C. L.; David, E.; Brickwood, J. R.; Schwartz, R.; Barringer, K. J.; Pauletti, D.; Shih, C.-K.; Erickson, D. A.; Sorge, C. L.; Joseph, D. P.; Hattox, S. E.; Adams, J.; Grob, P. M. Novel nonnuceloside inhibitors of HIV-1 reverse transcriptase. 7. 8-Arylethyldipyridodiazepinones as potent broad-spectrum inhibitors of wild-type and mutant enzymes. *J. Med. Chem.* **1998**, *41*, 2960–2971. (b) Cywin, C. L.; Klunder, J. M.; Hoermann, M.; Brickwood, J.; David, E.; Grob, P. M.; Schwartz, R.; Pauletti, D.; Barringer, K. J.; Shih, C.-K.; Sorge, C. L.; Erickson, D. A.; Hattox, S. E. Novel nonnuceloside inhibitors of HIV-1 reverse transcriptase. 7. 8-Aryloxymethyl and 8-arylthiomethydipyridodiazepinones. *J. Med. Chem.* **1998**, *41*, 2972–2984.

(17) Zhao, Z.; Wolkenberg, S. E.; Lu, M.; Munshi, V.; Moyer, G.; Feng, M.; Carella, A. V.; Ecto, L. T.; Gabryelski, L. J.; Lai, M.-T.; Prasad, S. G.; Yan, Y.; McGaughey, G. B.; Miller, M. D.; Lindsley, C. W.; Hartman, G. D.; Vacca, J. P.; Williams, T. M. Novel indole-3-sulfonamides as potent HIV non-nucleoside reverse transcriptase inhibitors (NNRTIs). *Bioorg. Med. Chem. Lett.* **2008**, *18*, 554–559.

(18) (a) Ragno, R.; Artico, M.; De Martino, G.; La Regina, G.; Coluccia, A.; Di Pasquali, A.; Silvestri, R. Docking and 3-D QSAR studies on indolyl aryl sulfones (IASs). Binding mode exploration at the HIV-1 reverse transcriptase non-nucleoside binding site and design of highly active *N*-(2-hydroxyethyl)carboxyamide and *N*-(2-hydroxyethyl)carboxyhydrazide derivatives. *J. Med. Chem.* **2005**, *48*, 213–223. (b) De Martino, G.; La Regina, G.; Ragno, R.; Coluccia, A.; Bergamini, A.; Ciaprini, C.; Sinistro, A.; Maga, G.; Crespan, E.; Artico, M.; Silvestri., R. Indolyl aryl sulfones (IASs) as HIV-1 non-nucleoside reverse transcriptase inhibitors. Synthesis, biological evaluation and binding mode studies of new derivatives at indole-2-carboxamide. *Antiviral Chem. Chemother.* **2006**, *17*, 59–77.

(19) Ragno, R.; Coluccia, A.; La Regina, G.; De Martino, G.; Piscitelli, F.; Lavecchia, A.; Novellino, E.; Bergamini, A.; Ciaprini, C.; Sinistro, A.; Maga, G.; Crespan, E.; Artico, M.; Silvestri, R. Design, molecular modeling, synthesis and anti-HIV-1 activity of new indolyl aryl sulfones. Novel derivatives of the indole-2-carboxamide. *J. Med. Chem.* **2006**, *49*, 3172–3184.

(20) Polinsky, A. Lead-likenss and Drug-likeness. In *The Practice of Medicinal Chemistry*, 3rd ed.; Wermuth C. G. Elsevier Ltd.: Oxford, U.K., 2008; pp 244−254.

(21) Veber, D. F.; Johnson, S. R.; Cheng, H.-C.; Smith, B. R.; Ward, K. W.; Kopple, K. D. Molecular properties influence the oral bioavilability of drug candidate. *J. Med. Chem.* **2002**, *45*, 2615–2623.

(22) The recombinant HIV-1 RT carrying the Y181I mutation was comparable to the Y181C substitution in terms of drug resistance, from an enzymological point of view. See ref 17.

(23) Corbett, J. W.; Rodgers, J. D. Discovery of second generation of quinazoline non-nucleoside reverse transcriptase inhibitors of HIV-1. *Prog. Med. Chem.* **2002**, *40*, 63–105.

(24) ALOGPS and ALOGpS values were calculated at the Web site www.vcclab.org using ALOGPS version 2.1: Tetko, I. V.; Gasteiger, J.; Todeschini, R.; Mauri, A.; Livingstone, D.; Ertl, P.; Palyulin, V. A.; Radchenko, E. V.; Zefirov, N. S.; Makarenko, A. S.; Tanchuk, V. Y.; Prokopenko, V. V. Virtual computational chemistry laboratory-design and description. *J. Comp. Aid Mol. Des.* **2005**, *19*, 453–463.

(25) VCCLAB, Virtual Computational Chemistry Laboratory. http://www.vcclab.org.

(26) (a) Silvestri, R.; La Regina, G.; De Martino, G.; Artico, A.; Befani, O.; Palumbo, M.; Agostinelli, E.; Turini, P. Simple, potent and selective pyrrole inhibitors of monoamine oxidase type A and type B. *J. Med. Chem.* **2003**, *46*, 917–920. (b) Silvestri, R.; Artico, M.; La Regina, G.; De Martino, G.; La Colla, M.; Loddo, R.; La Colla, P. Anti-HIV-1 activity of pyrryl aryl sulfone (PAS) derivatives. Synthesis and SAR studies of novel esters and amides at the position 2 of the pyrrole nucleus. *Farmaco* **2004**, *59*, 201–210. (c) Silvestri, R.; Marfè, G.; Artico, M.; La Regina, G.; De Martino, G.; Lavecchia, A.; Novellino, E.; Morgante, E.; Di Stefano, C.; Catalano, G.; Filomeni, G.; Abruzzese, E.; Ciriolo, M. R.; Russo, M. A.; Amadori, S.; Cirilli, R.; La Torre, F.; Sinibaldi Salimei, P. Pyrrolo[1,2-*b*][1,2,5]benzothiadiazepines (PBTDs): a new class of agents endowed with high apoptotic activity in chronic myelogenous leukemia K562 cells and in cells from patients at onset and imatinib-resistant. *J. Med. Chem.* **2006**, *49*, 5840–5844.

(27) La Regina, G.; Coluccia, A.; Silvestri, R. Looking for an active conformation of the future HIV-1 non-nucleoside reverse transcriptase inhibitors. *Antiviral Chem. Chemother.* **2010**, *20*, 231–237.

(28) Goodsell, D. S.; Morris, G. M.; Olson, A. J. Automated docking of flexible ligands: applications of AutoDock. *J. Mol. Recognit.* **1996**, *9*, 1–5.

(29) Korb, O.; Stützle, T.; Exner, T. E. PLANTS: Application of Ant Colony Optimization to Structure-Based Drug Design. In *Ant Colony Optimization and Swarm Intelligence*, Proceedings of the 5th International Workshop, ANTS; Dorigo, M., Gambardella, L. M., Birattari, M., Martinoli, A., Poli, R., Stützle, T., Eds.; Lecture Notes in Computer Science, Series 4150; Springer: Berlin, 2006; pp 247−258.

(30) *FlexX* version 2.2; BioSolveIT GmbH: Sankt Augustin, Germany; http://www.biosolveit.de/FlexX/.

(31) *Molecular Operating Environment (MOE)* version 2009.10; Chemical Computing Group Inc.: Montreal, Canada; http://www.chemcomp.com/.

(32) Zhao, Z.; Wolkenberg, S. E.; Lu, M.; Munshi, V.; Moyer, G.; Feng, M.; Carella, A. V.; Ecto, L. T.; Gabryelski, L. J.; Lai, M.-T.; Prasad, S. G.; Yan, Y.; McGaughey, G. B.; Miller, M. D.; Lindsley, C. W.; Hartman, G. D.; Vacca, J. P.; Williams, T. M. Novel indole-3-sulfonamides as potent HIV non-nucleoside reverse transcriptase inhibitors (NNRTIs). *Bioorg. Med. Chem. Lett.* **2008**, *18*, 554–559.

(33) Kohlstaedt, L. A.; Wang, J.; Friedman, J. M.; Rice, P. A.; Steitz, T. A. Crystal structure at 3.5 Å resolution of HIV-1 reverse transcriptase complexed with an inhibitor. *Science* **1992**, *256*, 1783–1790.

(34) Das, K.; Bauman, J. D.; Clark, A. D., Jr.; Frenkel, Y. V.; Lewi, P. J.; Shatkin, A. J.; Hughes, S. H.; Arnold, E. High-resolution structures of HIV-1 reverse transcriptase/TMC278 complexes: strategic flexibility explains potency against resistance mutations. *Proc. Nat. Acad. Sci. U.S.A.* **2008**, *105*, 1466–1471.

(35) Ren, J.; Milton, J.; Weaver, K. L.; Short, S. A.; Stuart, D. I.; Stammers, D. K. Structural basis for the resilience of efavirenz (DMP-266) to drug resistance mutations in HIV-1 reverse transcriptase. *Structure* **2000**, *8*, 1089–1094.

(36) Ren, J.; Nichols, C. E.; Chamberlain, P. P.; Weaver, K. L.; Short, S. A.; Stammers, D. K. Crystal structures of HIV-1 reverse transcriptases mutated at codons 100, 106 and 108 and mechanisms of resistance to non-nucleoside inhibitors. *J. Mol. Biol.* **2004**, *336*, 569–578.

(37) Ren, J.; Nichols, C. E.; Chamberlain, P. P.; Weaver, K. L.; Short, S. A.; Chan, J. H.; Kleim, J. P.; Stammers, D. K. Relationship of potency

and resilience to drug resistant mutations for GW420867X revealed by crystal structures of inhibitor complexes for wild-type, Leu100Ile, Lys101Glu, and Tyr188Cys mutant HIV-1 reverse transcriptases. *J. Med. Chem.* **2007**, *50*, 2301–2309.

(38) Ren, J.; Nichols, C.; Bird, L.; Chamberlain, P.; Weaver, K.; Short, S.; Stuart, D. I.; Stammers, D. K. Structural mechanisms of drug resistance for mutations at codons 181 and 188 in HIV-1 reverse transcriptase and the improved resilience of second generation non-nucleoside inhibitors. *J. Mol. Biol.* **2001**, *312*, 795–805.

(39) Code "scoring.svl" was obtained from SLV Exchange Web site http://svl.chemcomp.com (Chemical Computing Group, Inc., Montreal, Canada).

(40) Case, D. A; Cheatham, T. E., III; Darden, T.; Gohlke, H.; Luo, R.; Merz, K. M., Jr.; Onufriev, A.; Simmerling, C.; Wang, B.; Woods, R. The Amber biomolecular simulation programs. *J. Comput. Chem.* **2005**, *26*, 1668–1688.

(41) Meagher, K. L.; Redman, L. T.; Carlson, H. A. Development of polyphosphate parameters for use with the AMBER force field. *J. Comput. Chem.* **2003**, *24*, 1016–1026.

(42) Wang, J.; Wang, W.; Kollman, P. A.; Case, D. A. Automatic atom type and bond type perception in molecular mechanical calculations. *J. Mol. Graph. Model.* **2006**, *25*, 247–260.

(43) Wang, J.; Wolf, R. M.; Caldwell, J. W.; Kollman, P. A.; Case, D. A. Development and testing of a general AMBER force field. *J. Comput. Chem.* **2004**, *25*, 1157–1174.

(44) *AmberTools* version 1.4; http://ambermd.org/#AmberTools.

(45) *PyMOL* version 1.2r1; DeLano Scientific LLC: San Carlos, CA http://www.pymol.org/.

(46) Van Nhien, A. N.; Tomassi, C.; Len, C.; Marco-Contelles, J. L.; Balzarini, J.; Pannecouque, C.; De Clercq, E.; Postel, D. First synthesis and evaluation of the inhibitory effects of aza analogues of TSAO on HIV-1 replication. *J. Med. Chem.* **2005**, *48*, 4276–4284.

(47) Pannecouque, C.; Daelemans, D.; De Clercq, E. Tetrazolum-based colometric assay for the detection of HIV replication inhibitors: revised 20 years latter. *Nat. Protoc.* **2008**, *3*, 427–434.

(48) Maga, G.; Amacker, M.; Ruel, N.; Hubsher, U.; Spadari, S. Resistance to nevirapine of HIV-1 reverse transcriptase mutants: loss of stabilizing interactions and thermodynamic or steric barriers are induced by different single amino acid substitutions. *J. Mol. Biol.* **1997**, *274*, 738–747.